



## Calhoun: The NPS Institutional Archive

---

Theses and Dissertations

Thesis Collection

---

2006-06

# Streamwise fluctuations of vortex breakdown at high Reynolds numbers

Connelly, Jonathan S.

Monterey, California. Naval Postgraduate School

---

<http://hdl.handle.net/10945/2767>



Calhoun is a project of the Dudley Knox Library at NPS, furthering the precepts and goals of open government and government transparency. All information contained herein has been approved for release by the NPS Public Affairs Officer.

**Dudley Knox Library / Naval Postgraduate School**  
**411 Dyer Road / 1 University Circle**  
**Monterey, California USA 93943**

<http://www.nps.edu/library>



# **NAVAL POSTGRADUATE SCHOOL**

**MONTEREY, CALIFORNIA**

## **THESIS**

**STREAMWISE FLUCTUATIONS OF VORTEX  
BREAKDOWN AT HIGH REYNOLDS NUMBERS**

by

Jonathan Stephen Connelly

June 2006

Thesis Advisor:

T. Sarpkaya

**Approved for public release; distribution is unlimited.**

THIS PAGE INTENTIONALLY LEFT BLANK

<b>REPORT DOCUMENTATION PAGE</b>			<i>Form Approved OMB No. 0704-0188</i>	
Public reporting burden for this collection of information is estimated to average 1 hour per response, including the time for reviewing instruction, searching existing data sources, gathering and maintaining the data needed, and completing and reviewing the collection of information. Send comments regarding this burden estimate or any other aspect of this collection of information, including suggestions for reducing this burden, to Washington headquarters Services, Directorate for Information Operations and Reports, 1215 Jefferson Davis Highway, Suite 1204, Arlington, VA 22202-4302, and to the Office of Management and Budget, Paperwork Reduction Project (0704-0188) Washington DC 20503.				
<b>1. AGENCY USE ONLY (Leave blank)</b>		<b>2. REPORT DATE</b> June 2006	<b>3. REPORT TYPE AND DATES COVERED</b> Master's Thesis	
<b>4. TITLE AND SUBTITLE:</b> ) Streamwise Fluctuations of Vortex Breakdown at High Reynolds Numbers			<b>5. FUNDING NUMBERS</b>	
<b>6. AUTHOR(S)</b> Connelly, Jonathan S.				
<b>7. PERFORMING ORGANIZATION NAME(S) AND ADDRESS(ES)</b> Naval Postgraduate School Monterey, CA 93943-5000			<b>8. PERFORMING ORGANIZATION REPORT NUMBER</b>	
<b>9. SPONSORING /MONITORING AGENCY NAME(S) AND ADDRESS(ES)</b> N/A			<b>10. SPONSORING/MONITORING AGENCY REPORT NUMBER</b>	
<b>11. SUPPLEMENTARY NOTES</b> The views expressed in this thesis are those of the author and do not reflect the official policy or position of the Department of Defense or the U.S. Government.				
<b>12a. DISTRIBUTION / AVAILABILITY STATEMENT</b> Approved for public release; distribution is unlimited.			<b>12b. DISTRIBUTION CODE</b>	
<b>13. ABSTRACT (maximum 200 words)</b> This thesis deals with the characterization of the dependence on the flow geometry of the streamwise fluctuations of the stagnation point of vortex breakdown in axisymmetric tubes and over delta wing aircraft. The statistical analysis presented herein shows that in an axisymmetric tube the 'darting' about the mean stagnation point are distributed normally for the two Reynolds numbers: $Re_D = 230,000$ and $300,000$ (independently of the Reynolds number in the range noted). The darting over a delta wing is not only non-Gaussian but also exhibits rather large localized fluctuations (Strouhal numbers ranging from 0.04 to 0.1), presumably due to the strong influence of the surrounding flow and the geometrical conditions: increase of circulation along the trailing edge, the abrupt separation of flow at the base of the delta wing, and other protuberances that emerge from the upper and lower surfaces of the wing (support elements in laboratory and stabilizers on delta wing aircraft). It is concluded that the behavior of vortex breakdown is strongly dependent on the surrounding geometry and that only experiments in axisymmetric tubes can provide the purest form of vortex breakdown for numerical simulations and analytical studies towards the understanding of the internal turbulence and its spectrum within the breakdown bubble for theoretical and industrial purposes.				
<b>14. SUBJECT TERMS</b> Vortex Breakdown, Turbulence, Stagnation Point Fluctuation, Swirling Flow			<b>15. NUMBER OF PAGES</b> 49	
			<b>16. PRICE CODE</b>	
<b>17. SECURITY CLASSIFICATION OF REPORT</b> Unclassified	<b>18. SECURITY CLASSIFICATION OF THIS PAGE</b> Unclassified	<b>19. SECURITY CLASSIFICATION OF ABSTRACT</b> Unclassified	<b>20. LIMITATION OF ABSTRACT</b> UL	

NSN 7540-01-280-5500

Standard Form 298 (Rev. 2-89)  
Prescribed by ANSI Std. Z39-18

THIS PAGE INTENTIONALLY LEFT BLANK

**Approved for public release; distribution is unlimited.**

**STREAMWISE FLUCTUATIONS OF VORTEX BREAKDOWN AT HIGH  
REYNOLDS NUMBERS**

Jonathan S. Connelly  
Ensign, United States Navy  
B.S., United States Naval Academy, 2005

Submitted in partial fulfillment of the  
requirements for the degree of

**MASTER OF SCIENCE IN MECHANICAL ENGINEERING**

from the

**NAVAL POSTGRADUATE SCHOOL  
June 2006**

Author: Jonathan Stephen Connelly

Approved by: Distinguished Professor T. Sarpkaya  
Thesis Advisor

Distinguished Professor Anthony J. Healey  
Chairman, Department of Mechanical and Astronautical  
Engineering

THIS PAGE INTENTIONALLY LEFT BLANK

## ABSTRACT

This thesis deals with the characterization of the dependence on the flow geometry of the streamwise fluctuations of the stagnation point of vortex breakdown in axisymmetric tubes and over delta wing aircraft. The statistical analysis presented herein shows that in an axisymmetric tube the 'darting' about the mean stagnation point are distributed normally for the two Reynolds numbers:  $Re_D = 230,000$  and  $300,000$  (independently of the Reynolds number in the range noted). The darting over a delta wing is not only non-Gaussian but also exhibits rather large localized fluctuations (Strouhal numbers ranging from 0.04 to 0.1), presumably due to the strong influence of the surrounding flow and the geometrical conditions: increase of circulation along the trailing edge, the abrupt separation of flow at the base of the delta wing, and other protuberances that emerge from the upper and lower surfaces of the wing (support elements in laboratory and stabilizers on delta wing aircraft). It is concluded that the behavior of vortex breakdown is strongly dependent on the surrounding geometry and that only experiments in axisymmetric tubes can provide the purest form of vortex breakdown for numerical simulations and analytical studies towards the understanding of the internal turbulence and its spectrum within the breakdown bubble for theoretical and industrial purposes.



THIS PAGE INTENTIONALLY LEFT BLANK

## TABLE OF CONTENTS

<b>I.</b>	<b>VORTEX BREAKDOWN .....</b>	<b>1</b>
<b>A.</b>	<b>INTRODUCTION.....</b>	<b>1</b>
1.	Background .....	1
2.	Forms of Vortex Breakdown.....	2
a.	<i>Helical Vortex Breakdown</i> .....	2
b.	<i>Spiral Vortex Breakdown</i> .....	4
c.	<i>Nearly Axisymmetric Recirculation Vortex Breakdown</i> .....	5
d.	<i>Conical Vortex Breakdown</i> .....	6
3.	Scope of the Present Work .....	7
<b>B.</b>	<b>PHENOMENA .....</b>	<b>8</b>
<b>C.</b>	<b>CONICAL VORTEX BREAKDOWN .....</b>	<b>11</b>
1.	Characteristics of Conical Vortex Breakdown.....	11
2.	Streamwise Oscillations of Conical Vortex Breakdown.....	12
<b>II.</b>	<b>EXPERIMENTAL EQUIPMENT AND PROCEDURES .....</b>	<b>17</b>
<b>A.</b>	<b>FLOW APPARATUS .....</b>	<b>17</b>
<b>B.</b>	<b>FLOW VISUALIZATION AND OBSERVATIONS .....</b>	<b>19</b>
<b>C.</b>	<b>DATA COLLECTION AND ANALYSIS .....</b>	<b>20</b>
<b>III.</b>	<b>STATISTICAL RESULTS .....</b>	<b>21</b>
<b>A.</b>	<b>GENERAL REMARKS .....</b>	<b>21</b>
<b>B.</b>	<b>DISCUSSION OF FINDINGS .....</b>	<b>23</b>
<b>C.</b>	<b>CONCLUSIONS AND RECOMMENDATIONS.....</b>	<b>30</b>
	<b>LIST OF REFERENCES .....</b>	<b>33</b>
	<b>INITIAL DISTRIBUTION LIST .....</b>	<b>35</b>

THIS PAGE INTENTIONALLY LEFT BLANK

## LIST OF FIGURES

Figure 1.	Double Helix vortex breakdown in a diverging tube. (After Sarpkaya 1971a) .....	3
Figure 2.	Spiral vortex breakdown in a diverging tube. (After Sarpkaya 1971a) .....	4
Figure 3.	Axisymmetric recirculation “bubble” vortex breakdown. (After Sarpkaya 1971a) .....	5
Figure 4.	Axisymmetric vortex breakdown with a laminar sheet surrounding the vortex breakdown. (After Sarpkaya 1971a) .....	6
Figure 5.	Conical vortex breakdown. (After Sarpkaya 1995.) .....	7
Figure 6.	(a) Top view rendering of a delta wing. The sweep angle is labeled. (After Hummel 1967) (b) Side view rendering of a delta wing showing angle of attack. (After LeMay 1990) .....	9
Figure 7.	Power Spectrum Density for (a) 450 data points at $Re_D=230,000$ , (b) 507 data points at $Re_D=300,000$ , (c) Non-dimensional Power Spectrum Density for $Re_D=230,000$ , and (d) Non-dimensional Power Spectrum Density for $Re_D=300,000$ . .....	14
Figure 8.	Tube-and-vane type flow apparatus for inducing vortex breakdown (From Novak 1998). .....	17
Figure 9.	Profile of test tube used (all dimensions are in millimeters). (After Novak and Sarpkaya 2000). .....	18
Figure 10.	Probability Density Function of fluctuations of breakdown for: (a) 26 degree and (b) 37 degree angle of attack. (After Menke 1996) .....	24
Figure 11.	Fluctuations of breakdown location: Mitchell’s results are labeled “current results” and are superimposed on Menke’s (1996) results. (After Mitchell 2000). .....	25
Figure 12.	Time history of breakdown locations for $Re_D=230,000$ . 500 data points (Top) and 1,000 data points (Bottom). .....	26
Figure 13.	Comparison of normalized data to a Gaussian distribution (a) $Re_D=230,000$ (b) $Re_D=300,000$ . .....	27
Figure 14.	Cumulative Probability Distribution for normalized fluctuations from the mean. (a) $Re_D=230,000$ and (b) $Re_D=300,000$ . .....	28
Figure 15.	Tube test section indicating the location of the mean stagnation point, $X_m$ , and the entrance diameter, $D$ . .....	29
Figure 16.	Comparison of normalized data, $X/D$ , to a Gaussian distribution (a) $Re_D=230,000$ (b) $Re_D=300,000$ . .....	30

THIS PAGE INTENTIONALLY LEFT BLANK

## **ACKNOWLEDGMENTS**

From my family to lifetime friends it is difficult to put into words the gratitude I have for these people.

To my family, I am grateful that you have given me both an imagination to dream and the tools to implement my ideas. You have always been a source of faith and conviction and in times of need your encouragement has carried me.

To the many teachers and mentors I have encountered, I cannot thank you enough for leading me through my education. The most influential people in my adult life have been a few determined Professors who exude fervor for life and learning.

I am especially thankful for the opportunity to work with my advisor, Distinguished Professor Sarpkaya, who has, through the past year, been a gleaming example of the astute persona developed from a lifetime of dedication to learning. His tireless leadership and mentoring prudently shaped my postgraduate education and I will not forget his many lessons and sincere advice as I start my naval career.

To Stacy, I am thankful for your love and support this past year. You have been the ideal friend and companion through this part of my life.

Finally, I thank God for watching over me through the past year and bringing this endeavor to fruition.

THIS PAGE INTENTIONALLY LEFT BLANK

# **I. VORTEX BREAKDOWN**

## **A. INTRODUCTION**

### **1. Background**

Vortex breakdown is a phenomenon that has been studied extensively both theoretically and experimentally, yet it remains one of the many such naturally occurring phenomena in fluid flows that has not yet been fully understood. As is the case of many other flows, researchers have not been able to acquire sufficient understanding of vortex breakdown over delta wings, in tubes, and in combustion chambers. Observations have been made that describe the fundamental behaviors of vortex breakdown using many different and varying experimental procedures and equipment. But prior to exploring these rather complex methods for categorizing vortex breakdown, it is important to acquire a rather basic understanding of the physics and forms of the flow through an investigation of the breakdown in tubes.

The most common tool for identifying structures in fluid flow is called flow visualization. Flow visualization encompasses introducing a visually contrasting agent, dye, into the flow in order to trace streamlines within the flow. In vortex breakdown (hence forth VB) the dye is injected through a port aligned with the axis of the vortex core. As the fluid progresses naturally toward the breakdown point, the dye defines the flow structures in the fluid. This kind of flow visualization enables one to describe various aspects of the flow that evade state of the art instrumentation such as laser Doppler velocimetry (LDV) and digital particle image velocimetry (DPIV) which are used to measure quantitative elements of the flow. Other such instrumentation is used for determining the real-time behavior of the flow as it applies to aspects of mixing in combustion chambers and lift and drag in aerodynamics.

The two fundamental parameters, in addition to geometrical variables, that govern the behavior of the flow are Reynolds and swirl numbers, defined by equations (1) and (2) respectively.

$$(1) \quad \text{Re}_D = \frac{U_0 D_0}{\nu}$$



$$(2) \quad \gamma = \frac{\Gamma}{U_0 D_0}$$

Where  $U_0$  is the mean axial velocity,  $D_0$  is the tube entrance diameter,  $\nu$  is the kinematic viscosity, and  $\Gamma$  is the circulation.

Because of the dependence of these parameters on geometry, they are oftentimes presented in different forms. As such, they serve as scaling parameters and can be used to compare data with those obtained by others. The current investigation employs a tube-and-vane-type apparatus that allows for the precise setting of the desired Reynolds and swirl numbers through the regulation of the flow rate and the adjustable vane angles. The combination of the flow visualization with the variability of these experimental conditions provides insight into what happens as VB occurs.

## 2. Forms of Vortex Breakdown

Understanding the forms of VB is important in determining specific characteristics and behaviors of the flow. It is also important to note the relationship between the form of the breakdown and the conditions that are present for that breakdown to occur, i.e. Reynolds and swirl numbers. The four major types of VB are the double helix, spiral, nearly axisymmetric recirculation, and conical breakdowns. Several combinations of these salient forms of breakdown also transpire to create a medley of structures interacting within the flow.

### *a. Helical Vortex Breakdown*

Understanding the major forms of VB demands an exploration of the literature that helped establish them. The double helix was first observed by Sarpkaya (1971a). He used a tube-and-vane-type apparatus with adjustable flow rate and vane angles to control the Reynolds number and swirl number. Dye injected along the centerline into the flow was observed to decelerate and expand into two thin triangular sheets that wrap around each other forming a double helix. This form gradually expands to the limits of the tube and breaks down into mild turbulence. Sarpkaya (1971b) notes that the double helix is highly unstable and reacts to internal and external disturbances.

For this reason Sarpkaya (1971b) states that the double helix may not be a form of vortex breakdown, but rather a “consequence of the instability of the prevailing flow to spiral disturbances.”

Figure 1 illustrates this form of VB. The double helix is uniquely different from the other forms of VB because the flow remains laminar throughout the breakdown. Figure 1 below shows the dye filament at the vortex core splitting into two triangular sheets that become intertwined upstream of the shearing point. The sheets expand and become thinner, making them susceptible to turbulent motions. It is only near the walls of the diverging tube that sheets become interrupted by turbulence.

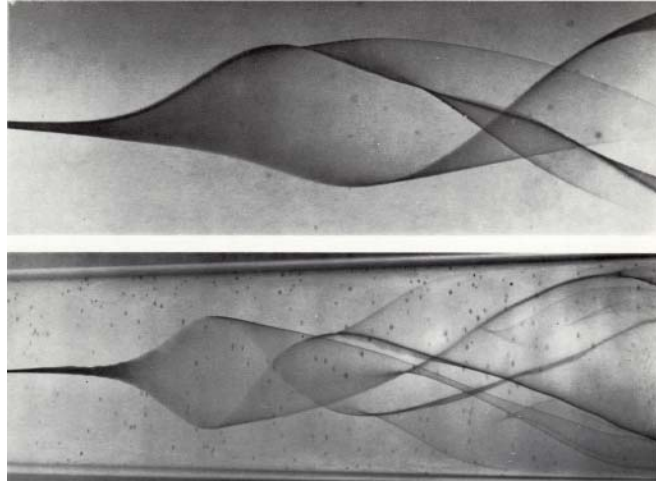


Figure 1. Double Helix vortex breakdown in a diverging tube. (After Sarpkaya 1971a)

The direction of the swirling flow is a consequence of the inception of the instability and of little importance to the breakdown. Both sheets curl in towards one another regardless of the direction of swirl. In the top figure of Figure 1 the sheets curl out of the page, while in the bottom figure the double helix is curling in the opposite direction. Because of the relatively low Reynolds numbers and high circulation numbers, reportedly  $Re < 2000$  and  $\Omega > 2.3$  from Sarpkaya (1971a), the double helix has only been observed in laboratory settings.

***b. Spiral Vortex Breakdown***

Spiral vortex breakdown is the next prominent type of vortex breakdown, occurring at Reynolds and swirl numbers slightly greater than those for the double helix form. Sarpkaya (1971a) reports that at constant Reynolds number of about 5,000 the vane angles can be increased to about 20 degrees to see the first indication of VB. By increasing the vane angle farther, the vortex core dye filament breakdown moves rapidly upstream and develops an abrupt kink that is indicative of rapid deceleration of the flow at the vortex core. After one or two windings the filament breaks up into large-scale turbulence. Figure 2 shows the spiral breakdown observed by Sarpkaya (1971a).

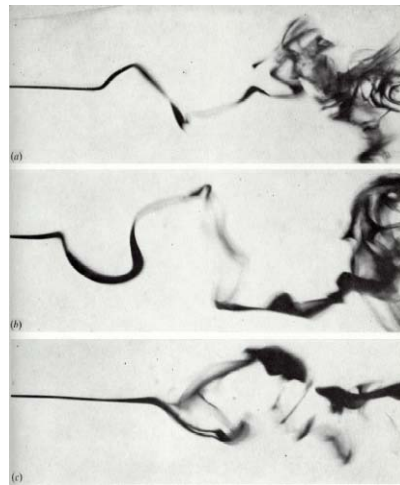


Figure 2. Spiral vortex breakdown in a diverging tube. (After Sarpkaya 1971a)

Figure 2 shows, from top to bottom, the effect of increasing the swirl. In each case, the nascent spiral is followed by large-scale turbulence. More detailed observations show that turbulent mixing increases along the length of the tube. It is also apparent from Figure 2 that the kink in the dye filament is not stationary. This unsteadiness is one of the behaviors of VB that is yet to be quantified. The changes in location of what may be called the stagnation point make the accurate quantification of time-averaged statistics rather difficult.

*c. Nearly Axisymmetric Recirculation Vortex Breakdown*

The characteristic shape of the axisymmetric recirculation form of VB is a 'bubble'. This description may be misleading to the casual reader, since shape and function of the shape are two separate entities. Therefore, it is best to introduce this form of VB with the help of a figure. Figure 3 shows what happens when the swirl is sufficiently increased. When the dye filament in the vortex core reaches the stagnation point it spreads around the outer shell of the bubble. Near the downstream limit of the shape, the dye is drawn into the recirculation portion of the bubble and becomes entrained there, as shown in the bottom figure of Figure 3.

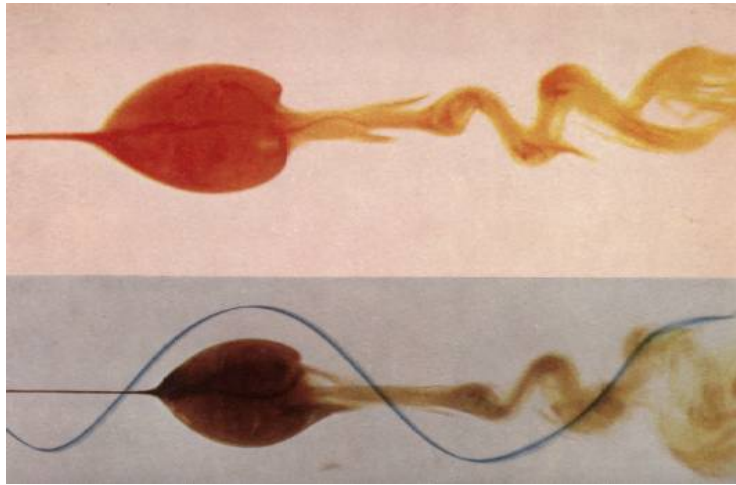


Figure 3. Axisymmetric recirculation “bubble” vortex breakdown. (After Sarpkaya 1971a)

It comes as no surprise that this kind of recirculation could be utilized in combustion processes to improve efficiency and to reduce combustion products. Lilley (1977) and Swithenbank and Chigier (1969) provide comprehensive reviews of the experimental work done in this field.

Unlike spiral VB, axisymmetric recirculation VB does not initiate large-scale turbulence in the adjacent regions. Figure 4 shows a sheet of dye that surrounds the bubble, expanding to accommodate the displaced volume of the bubble and converging again after the bubble.



Figure 4. Axisymmetric vortex breakdown with a laminar sheet surrounding the vortex breakdown. (After Sarpkaya 1971a)

#### *d. Conical Vortex Breakdown*

In 1995, a fourth form of VB was discovered and investigated by Sarpkaya (1995). Since then the conical VB has been the focus of the most recent research in the field. Occurring at high Reynolds numbers in noncavitating, turbulent, swirling flows, this type of breakdown exhibits a clear stagnation point followed by an axisymmetric expanding cone. Sarpkaya's (1995) observations show a small area of recirculation immediately after the stagnation point that bursts into a conical spiraling wake. By increasing the Reynolds number based on the tube diameter to 200,000 and adjusting the circulation number, he was able to eliminate the axisymmetric recirculation before the cone. Figure 5 shows the progression of the VB with increasing Reynolds number. The Reynolds numbers are 50 000, 100 000, 150 000, and 200 000 for the top to bottom pictures respectively. The corresponding circulation numbers are 0.77, 0.61, 0.55, and 0.50 from the top to the bottom picture, respectively.

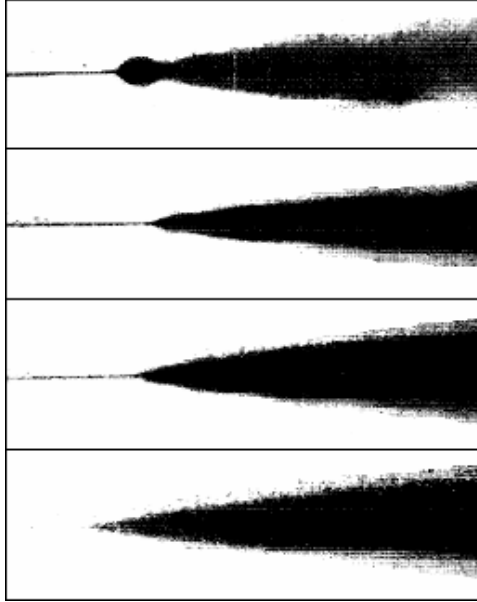


Figure 5. Conical vortex breakdown. (After Sarpkaya 1995.)

Novak and Sarpkaya (2000) discuss two phenomena that occur with the conical VB, vortex core meandering and stagnation point darting. The first, vortex core meandering, occurs when the core visibly moves radially about the mean centerline. Novak and Sarpkaya (2000) state that, when collecting data using an LDV, core meandering creates a region where turbulence measurements become unreliable. The darting of the stagnation point of the conical VB is the second phenomena and will encompass the bulk of the discussion in this thesis. It is a random streamwise fluctuation of the location of the VB, with no noticeable transition time or periodic motion. There is however a mean location for the stagnation point and a normal distribution of the axial displacements from the mean, as shown later.

### 3. Scope of the Present Work

So far the discussion has focused primarily on experimental flow visualization results from tube-and-vane type apparatus to describe VB. Vast amounts of data exist that examine time-averaged flows and provide conclusions that relate experimental results to applicable real life scenarios. By utilizing such results, engineers are able to design control systems in platforms such as the delta wing to provide for safer operation and enhanced maneuverability. The present study is aimed at furthering the bank of

knowledge that engineers have to work with. By understanding the behavior of the darting of the stagnation point of VB, engineers should be able to take one step closer to developing a safe operating envelop for the delta wing aircraft.

## **B. PHENOMENA**

Experiments dealing with the fluctuations of VB over delta wings have shown that a large number of parameters must be taken into consideration to understand the sources as well as the physics of the phenomenon. These include, but are not limited to, the sweep angle, leading-edge geometry, wing thickness, angle of attack, and the free-stream conditions. On the other hand, the fluctuations of VB in tubes are controlled by fewer parameters such as the Reynolds number and the circulation of the upstream vortex. There are, to be sure, secondary influences such as the boundary layer growth on the tube wall and the effect of air bubbles for the experiments conducted using water as the working fluid. Nevertheless, the tube experiments provide a clearer understanding of the characteristics of VB in general and of the streamwise fluctuations in particular. Furthermore, the effect of the boundary layer and the dissolved air can easily be minimized by the slight expansion of the tube wall, by de-aerating the water before introducing it into the test chamber, and by conducting the experiments under sufficiently high pressure, as in the case of the experiments reported herein. These will be discussed in greater detail later following a brief summary of the delta wing experiments.

For delta wings, the sweep angle and angle of attack are two of the parameters that determine where the VB occurs. Sweep angle is a measurement of the angle the leading edge makes with a line perpendicular to the axis of the delta wing that passes through the apex. Aspect ratio (the ratio of the wing span squared to the area of the wing) is another way to represent the sweep angle. Figure 6(a) is provided for clarification of the sweep angle. Figure 6(b) shows the angle of attack as the angle measured from the plane in the direction of the freestream fluid motion, usually the horizontal plane, to the bottom surface of the delta wing.

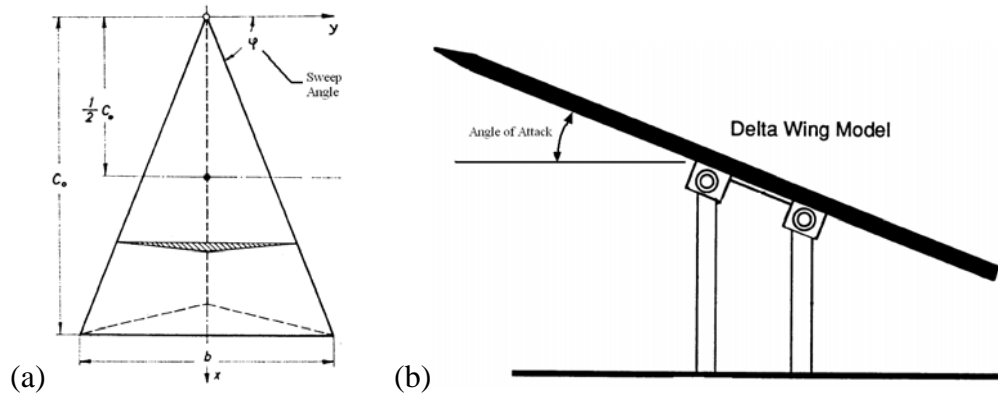


Figure 6. (a) Top view rendering of a delta wing. The sweep angle is labeled. (After Hummel 1967) (b) Side view rendering of a delta wing showing angle of attack. (After LeMay 1990)

Mitchell (2000) observed that “increasing angle of attack adds energy to the leading-edge vortices as a result of increased adverse pressure gradients producing higher axial and swirl velocities than at lower incidence angles.” The breakdown responds to these increased axial and swirl velocities by moving upstream towards the apex as the angle of attack is increased. Sarpkaya (1971a) observed similar events in a tube when increasing the vane angle to increase swirl. In his tube-vane-type apparatus, the increase in swirl resulted in an axial upstream displacement of the vortex breakdown.

Wentz (1971) found that increasing sweep angle would increase the angle of attack necessary for breakdown to occur. At a threshold of 75 degrees, the sweep angle was determined to have no effect on the angle of attack for breakdown to occur. Wentz (1971) also stated that no breakdown was observed for a sweep angle of 45 degrees at any angle of attack and at sweep angles of 50 and 55 degrees the breakdown never reached the trailing edge. This puts into focus that delta wings with sweep angles of greater than 55 degrees will experience VB over their wings, resulting in changes to lift, drag, and maneuverability. Evidently, the frequency and amplitude of the fluctuations of the location of the breakdown can be critical for stability of delta wing aircraft.

One critical angle of attack will be the angle of attack where the VB occurs over the trailing edge of the aircraft. Hummel (1967) and Mitchell (2000) discuss the conditions for the VB to occur over the delta wing in detail. Results from both studies show that as the sweep angle is increased, the angle of attack for VB to occur over the



wing also increases. Mitchell's (2000) results also show that as the freestream velocity increases, the angle of attack for VB to occur over the wing increases. Thus, it may be concluded that an increase in freestream velocity and/or sweep angle will increase the necessary angle of attack for VB to occur over delta wings.

Hummel's (1967) investigation also includes results for the lift, drag, and pitching moment coefficients. Once the VB crosses the trailing edge and is over the wing, there is a marked decrease to these coefficients. As the breakdown moves toward the apex, the condition becomes more serious and the delta wing begins to experience stalling. Hummel (1967) concluded that "at larger aspect ratios, the effect of vortex breakdown starts at lower values of the angle of incidence." This conclusion is complimentary to the one made previously and simply states that as the sweep angle is decreased (aspect ratio increases) the VB will cross the trailing edge at a smaller angle of attack.

Menke (1996) offered further validity to the discussion of Reynolds number dependence by noting that in his frequency analysis the amplitude of the dominant frequency of the darting of the stagnation point was smaller at lower Reynolds numbers. This study also investigated the amplitude of trailing edge pressure fluctuations for three mean breakdown locations, at the trailing edge, near the apex, and at the mid-point. Understanding the pressure fluctuations leads to an understanding of the stability of the aircraft. For the breakdown over the trailing edge, the least amount of fluctuation was observed. When the breakdown was over the mid-point, pressure fluctuations at the trailing edge increased to two or three times the magnitude of those observed for breakdown over the trailing edge. The highest fluctuation of pressure at the trailing edge was observed for breakdown close to the apex. These fluctuations were two to three times larger than those for the mid-point. As these fluctuations increase instability of and loss of control of the aircraft are more likely to occur. Menke (1996) also investigated the distribution of the fluctuations of the breakdown location based on two angles of attack. The results were presented as a histogram and a probability density function. Menke (1996) concluded that his results were not normally distributed when compared to a Gaussian curve. The consequence of this finding is that the fluctuation in VB is neither periodic nor normally distributed. This point will be taken up again in connection with the discussion of the tube experiments.

Menke (1996) also investigated the interaction of the vortices occurring on opposite leading edges. He stated that “there is an antisymmetric motion of breakdown location for left and right vortices.” Both breakdowns oscillate at about the same frequency separated by a phase angle of approximately 180 degrees. Mitchell (2000) noted that there are strong interactions between the leading edge vortices, such that “as the breakdown location on one side of the delta wing moves aft, the other tends to move forward and vice versa.” Both Mitchell (2000) and Menke (1996) are in agreement that in some instances the oscillations are 180 degrees out of phase.

The brief summary here illustrates the complexity of experimentation with models of delta wing aircraft. Quite simply it is the shape of the delta wing and the variability of the phenomena that makes the measurements difficult. What is even more difficult is developing a clear understanding of the physics of the fluid motion. That is why the remainder of this discussion will be focused on breakdown in tubes.

## **C. CONICAL VORTEX BREAKDOWN**

### **1. Characteristics of Conical Vortex Breakdown**

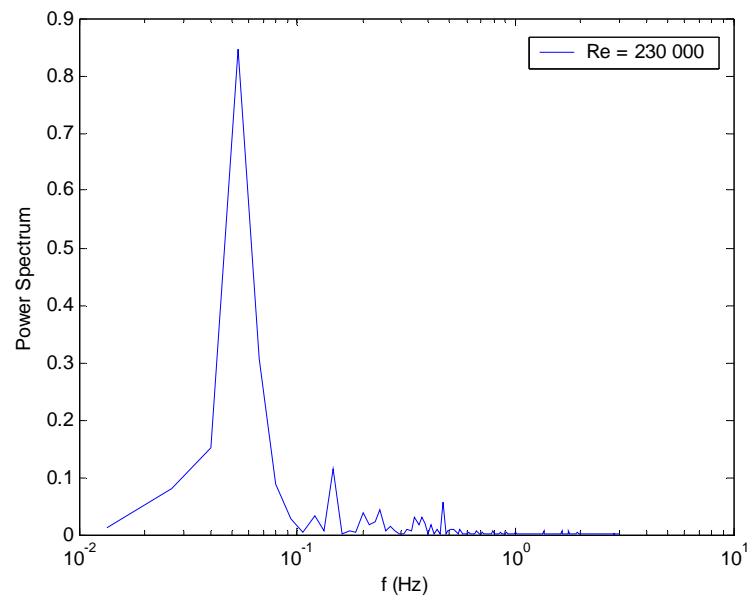
In the foregoing we have discussed the fundamental forms of VB. We have stated that where it occurs, why it occurs, and what happens when it occurs are questions that have only been answered partially. Of the forms discussed only the conical VB (CVB) will be examined here to uncover answers to these questions. CVB owes its occurrence to high Reynolds number but not necessarily to high circulations. The fact that it does not occur at a fixed point in a tube nor on a delta wing is the reason for the work described here in. Our purpose was to understand this aspect of CVB to the extent possible through the analysis of high speed motion pictures depicting the motion of CVB and carrying out a thorough statistical analysis to uncover the physics of the phenomena. These results will subsequently be compared with those obtained on delta wings at various Reynolds numbers.

As shown in Figure 5, CVB starts from a stagnation point and expands conically toward the limits of the tube. In the case of flow over a delta wing, the limits are determined by geometry, Reynolds number, and angle of attack to name a few. Because

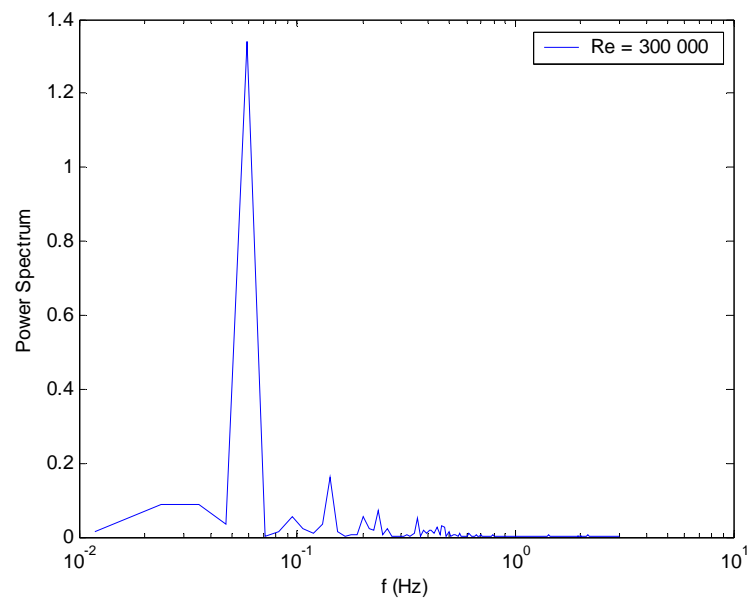
of the nature of this flow it is no longer possible to identify spatially coherent structures within the breakdown region. What is seen are only various scales of micro to macro turbulence emerging from the stagnation point. The stagnation point itself is at an instant a location from which CVB originates, however its location is not stagnant in the strict sense of the word. Like the flow inside the cone, the stagnation point location is constantly changing. It will be shown later, however, that there is order to the chaos in the stagnation point location, giving physical meaning to the CVB phenomena.

## **2. Streamwise Oscillations of Conical Vortex Breakdown**

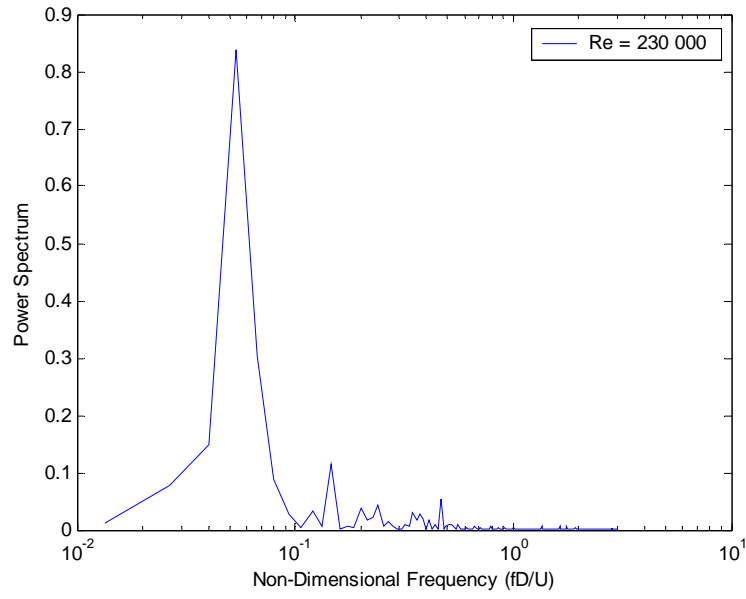
This study examines CVB at two Reynolds numbers,  $Re_D=230\,000$  and  $300\,000$ , in a diverging tube. The circulation was adjusted such that the mean location of the breakdown was within the test section, but not to the point for cavitation to occur in the flow. The apparatus was also pressurized to maintain sufficient static pressure to prevent cavitation. Aside from cavitation, there are other external factors that require considerable attention and are worth noting. Because the flow was driven by a high volume pump, the variation in electrical input and water pressure could cause noticeable deviation in results if that variation was sufficiently large. Because the temporal average of velocities and turbulence intensities were taken over relatively long periods, small variations in electrical input and water pressure would not present a notable discrepancy in the results. It can also be reasoned that in the case of larger external variations, the response of the VB would be significant enough to be eliminated on the basis of it being an outlier in the data. In the moderate case that an external disturbance was promulgated to the results, an analysis of the frequency spectrum would help separate the noise from the actual behavior of the VB. Figure 7 shows the power spectrum density for the darting of the stagnation point of CVB.



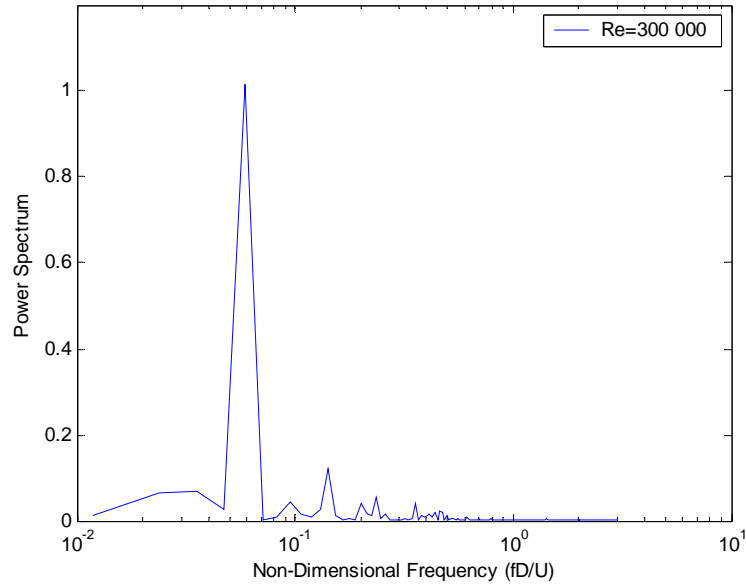
(a)



(b)



(c)



(d)

Figure 7. Power Spectrum Density for (a) 450 data points at  $Re_D=230,000$ , (b) 507 data points at  $Re_D=300,000$ , (c) Non-dimensional Power Spectrum Density for  $Re_D=230,000$ , and (d) Non-dimensional Power Spectrum Density for  $Re_D=300,000$ .

When compared to results in the literature from Menke (1996) and Mitchell (2000), whose experiments were conducted over delta wing models, the peak frequency for the oscillations occur at the same non-dimensional frequency or Strouhal number range, from 0.04 to 0.1, as seen in Figure 7(c) and (d). The absence of any large peaks at higher frequency in Figure 7(a) and (b), such as 60 Hz for electricity, indicates that the CVB fluctuation is free from such external disturbances.

THIS PAGE INTENTIONALLY LEFT BLANK

## II. EXPERIMENTAL EQUIPMENT AND PROCEDURES

### A. FLOW APPARATUS

The flow apparatus consisted of a removable Plexiglas tube, the vane section, the foam baffle, steel outer chamber with four windows, inlet and outlet ports, and a concave centerbody as shown in Figure 8 (for additional details see Novak 1998).

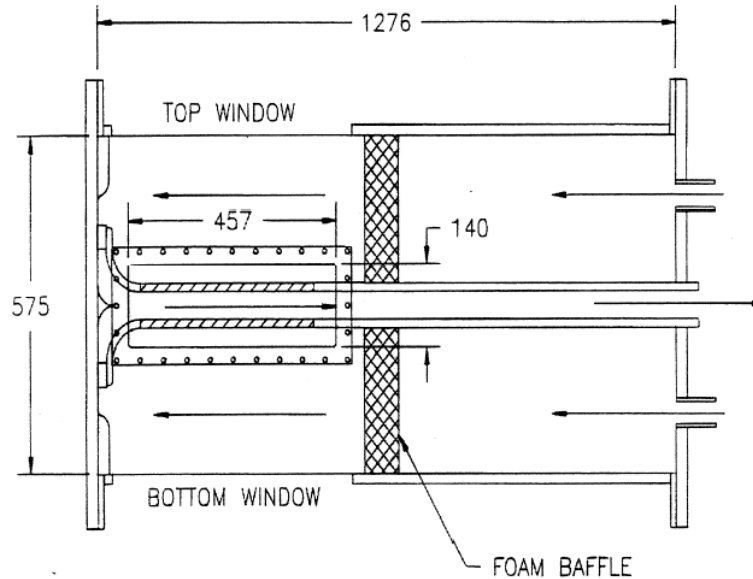


Figure 8. Tube-and-vane type flow apparatus for inducing vortex breakdown (From Novak 1998)

Other requisite elements were the centrifugal pump, air escape lines, flow meters, and a 12 m<sup>3</sup> reservoir. Each of these parts was vital in maintaining steady conditions for the VB to occur. Because the working fluid was water, eliminating air bubbles and cavitation became a design consideration when working at high Reynolds numbers. Another design consideration was the development of a boundary layer on the inner surface of the tube.

Because of the possibility of cavitation and for air bubbles to form, the steel outer chamber was constructed to withstand high static pressures. Sufficient static pressure was maintained in the apparatus to prevent cavitation by controlling the flow rates at the inlet and outlet. Additionally, air was periodically purged from the system to reduce the occurrence of bubbles in the test section.



Since a developing boundary layer on the inner surface of the tube was unavoidable, the tube was designed to account for the displacement thickness of the boundary layer by diverging at a 1.4 degree angle. This prevented the core flow from being adversely effected by the developing boundary layer. Figure 9 is a rendering of the tube used in the present study.

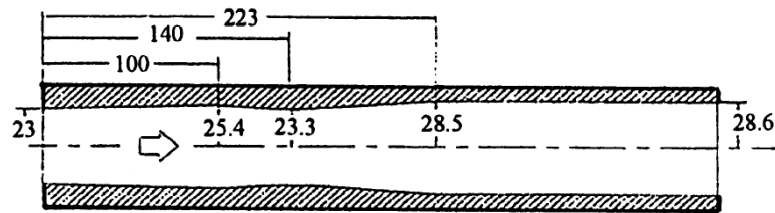


Figure 9. Profile of test tube used (all dimensions are in millimeters). (After Novak and Sarpkaya 2000)

More specifically, the tube depicted in Figure 9, starts at the inlet radius of 23 mm, diverges to a radius of 25.4 mm, and then converges to a throat with a radius of 23.3 mm located at 140 mm from the entrance. From this point, the tube rapidly diverges to a 28.5 mm radius at 223 mm from the inlet and then gently diverges at 1.4 degrees to the final diameter of 28.6 mm. This tube was machined from a solid three inch Plexiglas rod. The factory finish was maintained on the outer surface, but the inner wall was machined to the desired profile, ground to eliminate sharp corners, and then polished to a mirror finish.

Another important part of the apparatus is the concave centerbody which facilitated the transition of swirling flow from the vanes into the test section. The centerbody was also the location of the two inlet ports for the flow visualization agents, food coloring and fluorescein. One port was located at the centerline so that dye could be injected into the vortex core and the other port was located slightly off the flow axis. It should be apparent that the port along the centerline was used to obtain flow visualization of the VB, which was of paramount importance, but the other port provided for observations of the behavior of the flow surrounding the VB.

The system was cleaned periodically. Before a new run commenced, the test tube was removed to facilitate cleaning of the inside wall and the vanes and bellmouth were also wiped clean. The water was also filtered through a 10 micron filter before and after the experiments to remove any particulate matter.

The apparatus described herein was an augmentation from that used by Sarpkaya (1971a, 1971b, 1974, 1995) and identical to that used by Novak and Sarpkaya (2000).

## **B. FLOW VISUALIZATION AND OBSERVATIONS**

The SVHS video that was analyzed for this thesis was recorded using a Sony Shoulder mounted camera at the standard speed of 30 frames per second for CVB with Reynolds numbers of 230,000 and 300,000. Once the correct flow rates were achieved, the vane angles were adjusted such that the CVB occurred in the field of view of the camera. The amount of dye introduced to the system through the center port was also carefully controlled so that the breakdown form was clear for the camera. Excess dye prohibited accurate measurements of the stagnation point, as did not enough dye. Lighting was also a factor. Medium diffuse back lighting was used to illuminate the vortex core and breakdown region.

At 30 frames per second it was nearly impossible to separate any part of the structure of the breakdown from the turbulent cone. It was also apparent that the entire breakdown structure moved as the stagnation point fluctuated, such that there was no obvious lag time or remnants from the previous breakdown locations. This observation is merely qualitative, but it illustrates that when the CVB occurs over a delta wing aircraft, the lift and drag characteristics of the aircraft would change instantaneously as the breakdown point changed location on the wing. To further refine the measurement of the CVB stagnation point some electronic means could have been used, but such an effort was not assumed because visual observation was possible. A potential topic for a future thesis could be the development of an electronic means for measuring the location of the stagnation point.

### **C. DATA COLLECTION AND ANALYSIS**

The video tapes were played back using a Panasonic AG-1980 SVHS Desktop Editor and a Panasonic TR-124MA video monitor and stopped every 5 frames to record the location of the stagnation point of the CVB using a ruler mounted to the monitor. 2000 data points were collected in this manner at each Reynolds number. Invariably the axial location of the stagnation point of the breakdown showed at least some movement in between each of these measurements.

It is necessary to note that there were several breaks in the video which prevented the collection of 2000 consecutive data points. However, since it seems that the fluctuations are at all times random this should not affect any statistical results. It is also necessary to discuss the uncertainty in the data collection process. Because the stagnation point of the vortex breakdown is the location where the conical form erupts from the vortex core, the exact location of the point of eruption is indeterminable and can only be estimated. This estimation became more difficult when the vortex core was enlarged due to the amount of dye being injected. But because the breakdown was conical, it was possible to trace the periphery of the breakdown toward the stagnation point to obtain a better estimate of its location. The uncertainty in these measurements was determined to be  $\sim 2.0$  mm on the measurement scale.

The mean of the measured fluctuations was calculated and then subtracted from each data point to give the fluctuations from the mean. Since the ruler scale was arbitrarily placed, it was necessary to convert the measured fluctuations from the ruler scale to actual distances for comparison with future studies. Consequently a scaling factor was calculated by taking the ratio of a distance measured on the ruler to the same distance measured on the scale in the video. Using the scaling factor, each measured fluctuation was subsequently converted to actual displacements from the mean. These fluctuations of the CVB, the darting of the stagnation point, were finally normalized by the tube entrance diameter. Statistical analysis of the normalized data was performed using Microsoft Excel and MATLAB to determine the physical behavior of the phenomena. The results are presented in the next chapter.

### **III. STATISTICAL RESULTS**

#### **A. GENERAL REMARKS**

This chapter deals with the results of the darting of the stagnation point of CVB in tubes and the distribution of these fluctuations for comparison with investigations carried out with delta wings and subsequently to discuss any similarities and differences of the delta wing case and the vortex tube case. One can anticipate that the position of the breakdown as well as the distribution of the fluctuations in the two said cases will not necessarily be the same. The fundamental differences are that in the case of swirl confined to a tube, total circulation throughout the length of the tube remains constant, where as in the case of delta wings the circulation of the vortex increases along its length from the apex to the tail section or until the point where the VB occurs. Thus the differences of the histories of the circulation are expected to influence not only the shape of the distribution of the stagnation point location but also the distance at which the breakdown occurs. In addition to the foregoing, one must point out additional factors which affect all of the characteristics (breakdown location, frequency of fluctuation, the distribution of the fluctuations, etc.) in the two cases.

For a delta wing the rolled up vortex is bounded by the upper surface of the wing and is otherwise free in all directions; the external pressure gradient remains the atmospheric pressure. However on the wing surface the swirling conical flow gives rise to oppositely-signed vorticity. Therefore the vorticity generated on the lower surface of the wing and curling up to a vortex on the upper surface increases, as stated earlier, with distance, but is also decreased (to a smaller extent) due to the vorticity generated at the upper surface. After nearly 50 years of research on VB it has not been possible to analytically predict the position of the breakdown, let alone its consequences. One can certainly state that the flow over the delta wing can not be the same as in a tube. From a practical point of view a delta wing is seldom free from protuberances, particularly at its upper surface, which interfere with the conical flow.

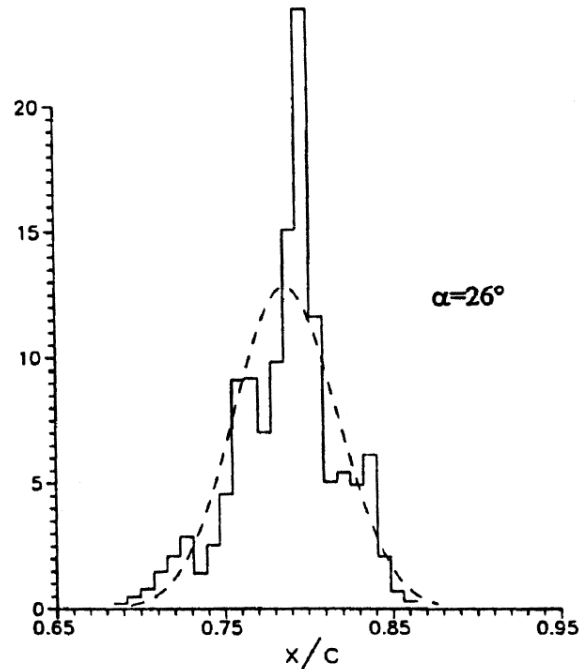
In the case of a tube, the circulation is constant even though the vorticity distribution varies first gradually as one approaches the stagnation point and rapidly at

and beyond the stagnation point as evidenced in the photographs shown in Figure 5. The tube walls are sufficiently far away from the vortex core (prior to breakdown) to account for the changes in vorticity and the effect of the pressure gradient is judiciously compensated by the slight expansion of the tube wall. Thus this makes the investigation of the fluctuations of VB in a tube relatively ideal and more physics based without trying to deal with other influencing factors such as the changes in the vorticity distribution, etc. as noted above. Consequently the creation of a mobile stagnation point and its fluctuation created by the occurrence of the breakdown, as better understood by the distribution, cannot be predicted because the transformation of a vortex with a very thin core into a swirling turbulent vortex with a large core and highly distributed vorticity with numerous orders of coherent structures leads to not only one but to a series of discrete frequencies.

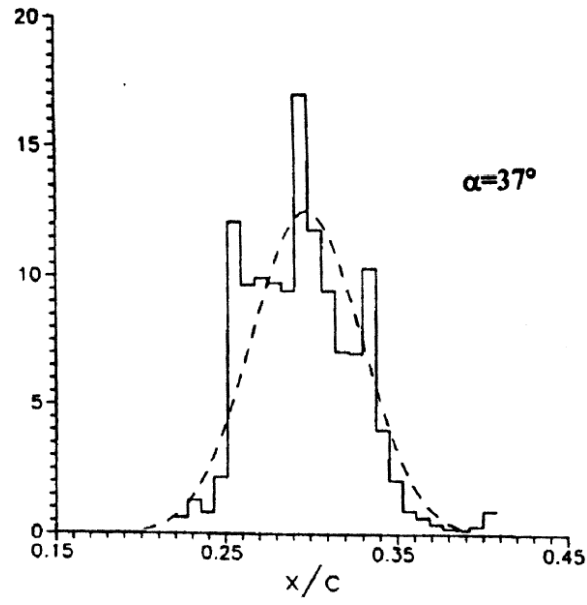
Comparison of the results of the delta wing studies with those obtained in a tube are far from obvious and had to be understood towards the understanding of the occurrence of the breakdown. One may conjecture, for example, that the breakdown location will exhibit both the high frequency fluctuations and then several lower frequencies due to the response of the large turbulent fluctuations of flow down stream of the breakdown. In fact, cold-flow experiments conducted in combustion chambers have shown that the shorter the length of the combustion chamber for a given diameter the larger the range of frequencies (Swithenbank and Chigier 1969). In the present experiments the full awareness of the numerous phenomena noted above dictated that the length of the tube downstream of the breakdown point be made sufficiently long ( $L/D \sim 27$ ) to eliminate Helmholtz resonance and additional frequencies. Furthermore the exit of the tube was varied numerous times to reduce such fluctuations. An additional consideration for the downstream section of the tube was that the conical breakdown fill the entire tube long before the end of the tube was reached so that essentially the flow became self-similar. It is on the basis of the foregoing that we will now discuss the results and compare them with those from delta wings.

## B. DISCUSSION OF FINDINGS

As expected the external influences on the evolution of the vortex over a delta wing exhibit fluctuations which are close enough to a Gaussian distribution but also exhibiting wilder fluctuations along the length of the vortex. It is a well known fact that part of the secondary fluctuations come from the variation of the breakdown location with the tail end of the wing. In other words when the VB momentarily moves downstream from its mean position it comes closer to the tail of the wing and thus is further influenced by its proximity. When the breakdown moves upstream (for random vorticity fluctuations) then the increase of the distance between the breakdown and the tail reduces the larger fluctuations. Evidently the extraneous influences are almost entirely eliminated in the case of our experiments. For example Menke's (1996) probability density function of fluctuations of breakdown locations over delta wings for angles of attack of 26 and 37 degrees are shown in Figure 10(a) and (b) respectively.



(a)



(b)

Figure 10. Probability Density Function of fluctuations of breakdown for: (a) 26 degree and (b) 37 degree angle of attack. (After Menke 1996)

The figure shows that the data is skewed toward the right of the Gaussian distribution (shown with dotted lines) at the relatively smaller angles of attack. However at very large angles of attack the tail proximity effects are so strong that the distribution comes not so surprisingly closer to a Gaussian distribution with at least three wild fluctuations.

In some cases the fluctuation distribution is not presented as a probability density function, but rather in the form histograms of the dominant frequencies, the power spectra density. Figure 11 shows Mitchell's (2000) presentation of his power spectra density results as compared to those of Menke (1996).

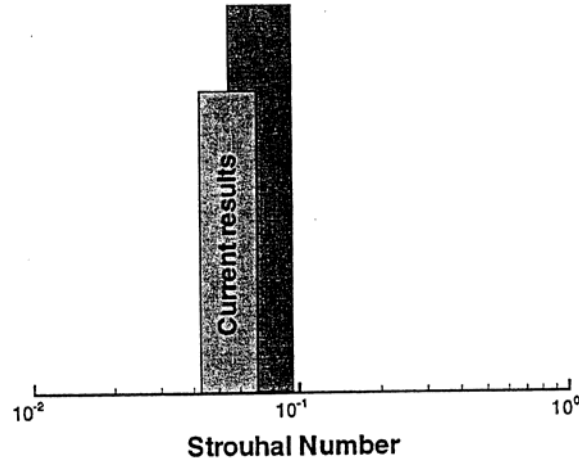


Figure 11. Fluctuations of breakdown location: Mitchell's results are labeled "current results" and are superimposed on Menke's (1996) results. (After Mitchell 2000)

The overlap of the results in these delta wing experiments are for Strouhal numbers of about 0.04 to 0.1. Gursul (1995) also has comparable results with peaks in the power spectra density at Strouhal numbers of 0.1, 0.06, and 0.08 for angles of attack of 37, 30 and 27 degrees respectively. When compared to the results from the present study in Figure 7 the correlation between the dominant frequency of fluctuations in a tube and over delta wings is evident for the stated Strouhal number range.

We will now discuss the results obtained in the present investigation in light of the foregoing. A critical investigation of the valuable statistical properties of CVB must start with an understanding of the time history of the breakdown location. Observation of video of the CVB reveals that the stagnation point of the breakdown is always changing location. As shown in Figure 12, the fluctuation has no apparent pattern and moves arbitrarily about the mean value, in this case the x-axis.



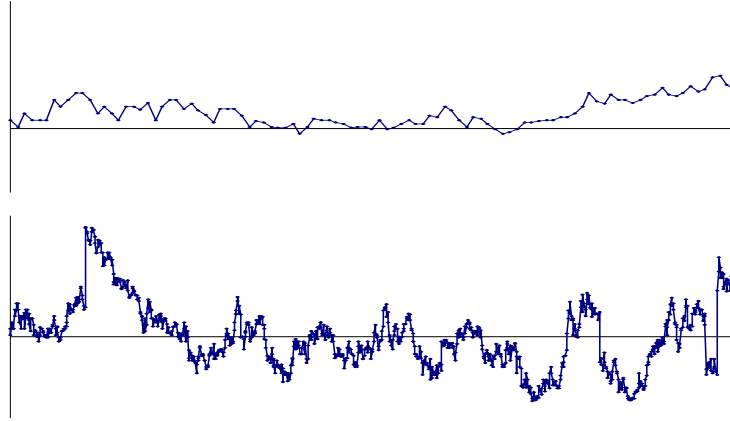
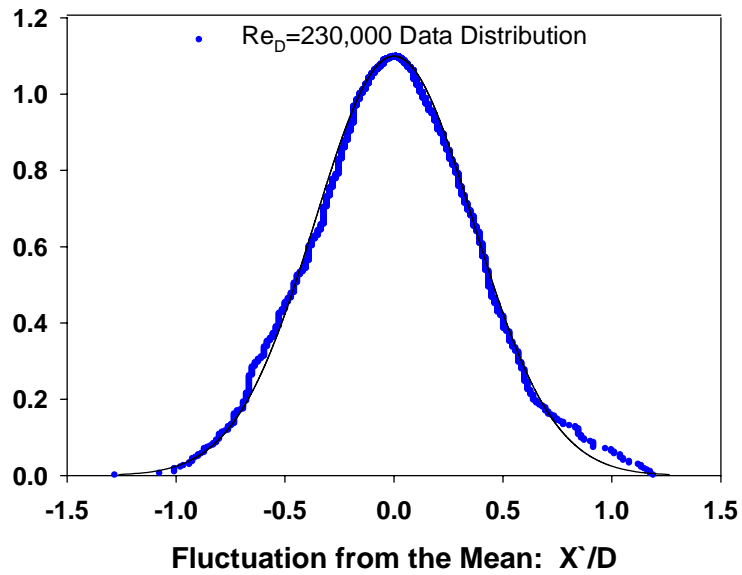


Figure 12. Time history of breakdown locations for  $Re_D=230,000$ . 500 data points (Top) and 1,000 data points (Bottom)

Figure 13 shows the results for the normalized fluctuation from the mean as compared with the Gaussian distribution.



(a)

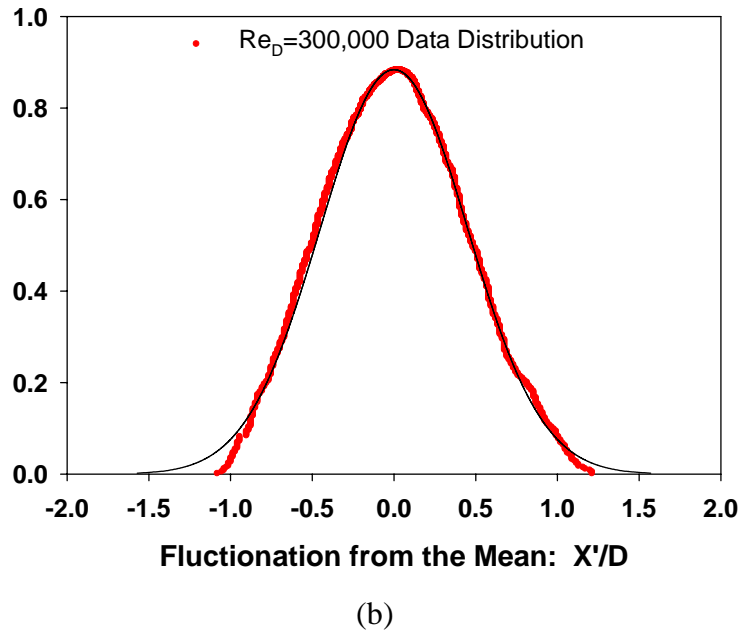
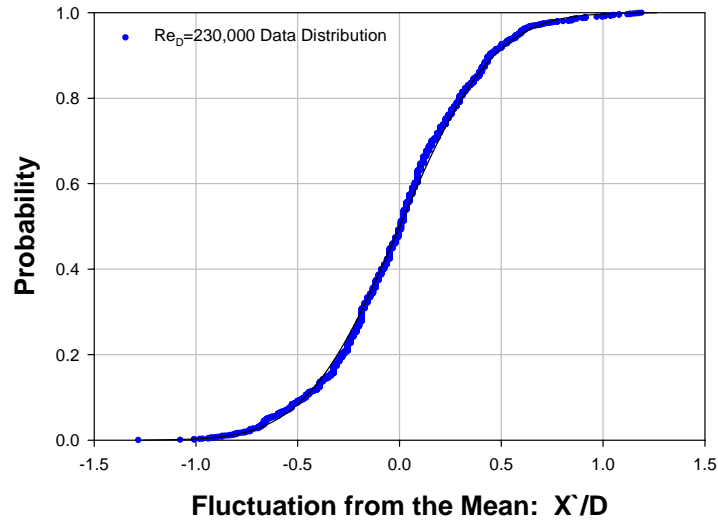
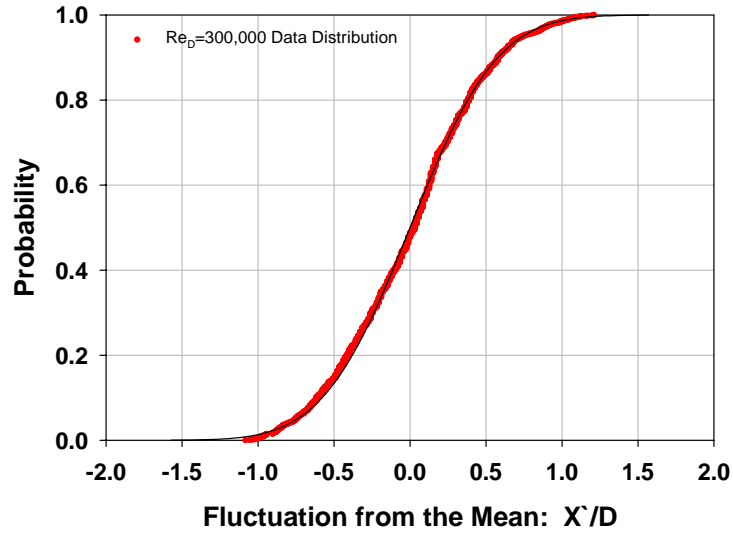


Figure 13. Comparison of normalized data to a Gaussian distribution (a)  $Re_D=230,000$  (b)  $Re_D=300,000$ .

Evidently these distributions are almost perfectly Gaussian except at the very tail ends showing the larger fluctuations are more apt to contain other frequencies than the smaller fluctuations. Figure 13 shows the non-dimensional fluctuation from the mean,  $\mu$ , where  $\mu=5.71e-4$  for  $Re_D=230,000$  and  $\mu=8.63e-16$  for  $Re_D=300,000$ . The standard deviation,  $\sigma$ , was  $\sigma=0.363$  for  $Re_D=230,000$  and  $\sigma=0.451$  for  $Re_D=300,000$ . Figure 14 shows that the cumulative probability distribution for both Reynolds numbers is very symmetric.



(a)



(b)

Figure 14. Cumulative Probability Distribution for normalized fluctuations from the mean. (a)  $Re_D = 230,000$  and (b)  $Re_D = 300,000$ .

The experiments were, as noted, carried out at two significantly different Reynolds numbers. The results show that at such high Reynolds numbers the effect of the Reynolds number is insignificant when protuberances are absent.

For a more complete understanding of the data presented here, the fluctuations will now be presented in the form  $(X_m + X')/D$  or  $X/D$ , where  $X_m$  is the mean stagnation point location,  $X'$  is the fluctuation from the mean, and  $D$  is the entrance diameter of the tube as shown in Figure 15.

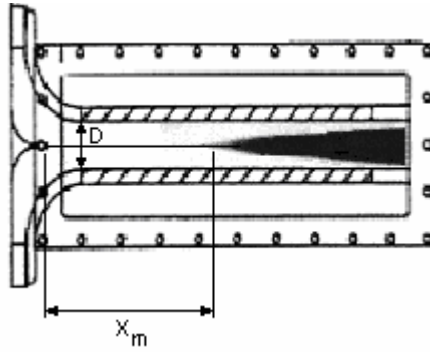
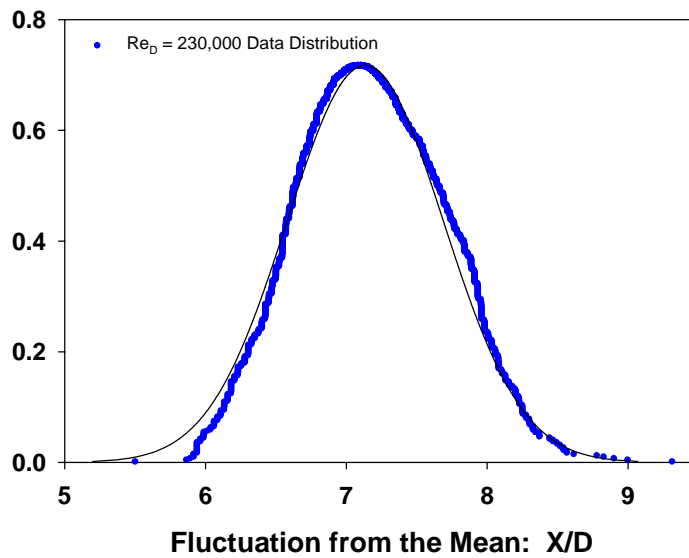
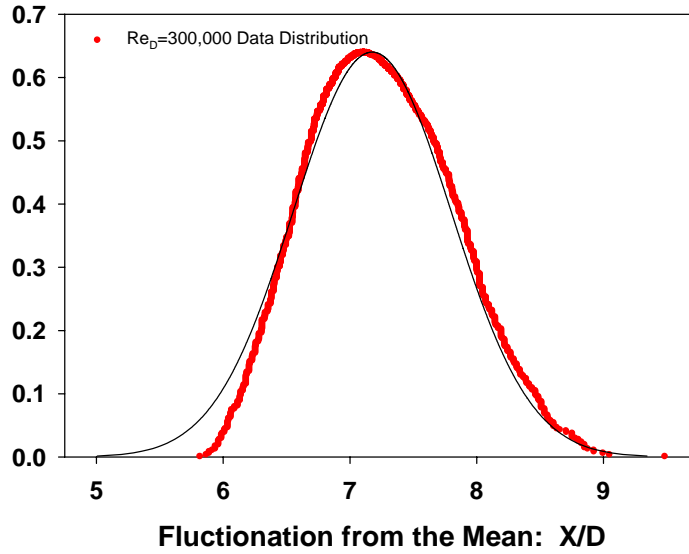


Figure 15. Tube test section indicating the location of the mean stagnation point,  $X_m$ , and the entrance diameter,  $D$ .

The distribution of the data for both Reynolds numbers is shown in Figure 16.



(a)



(b)

Figure 16. Comparison of normalized data,  $X/D$ , to a Gaussian distribution (a)  $Re_D=230,000$  (b)  $Re_D=300,000$ .

Note that the mean and standard deviation change to  $\mu=7.134$  and  $\sigma=0.556$  for  $Re_D=230,000$  and  $\mu=7.176$  and  $\sigma=0.623$  for  $Re_D=300,000$ . The shapes of the distributions are nearly Gaussian and both are slightly skewed to the left. These results do however resemble the previously presented results from Figure 13 and support the conclusion that the darting of the stagnation point is normally distributed.

### C. CONCLUSIONS AND RECOMMENDATIONS

It has been shown that conical vortex breakdown exhibits streamwise fluctuations in the location of the stagnation point that are arbitrary and naturally occurring. The frequencies at which these fluctuations occur in tubes are identical to those found in the delta wing cases, validating this study as a positive contribution to the bank of knowledge to include other such phenomena and physical attributes of vortex breakdown. After nearly 50 years of research on vortex breakdown, to include theoretical, numerical, and experimental investigations, it is the case that this phenomenon has been limited to and remains largely in the realm of qualitative observation. The complex geometries and

protuberances in delta wing aircraft make it difficult to accurately predict the instantaneous location of the stagnation point and since the history of the breakdown plays a decisive role in the movement of the breakdown as well as the interaction of the two leading edge vortices, which are formed on the wings of the delta wing, prediction of the breakdown location is at this time too complex and involves too many variables. Experiments in tubes have provided robust results and should be depended upon for comparison with future numerical simulations. As computational methods become more advanced and models are developed to predict high Reynolds number, turbulent, swirling flows the physical limitations in measurement techniques of vortex breakdown should no longer be an obstacle. However, until this definitive point is reached, the efforts of innumerable researchers using various methods will encompass the basis of understanding of vortex breakdown.

THIS PAGE INTENTIONALLY LEFT BLANK

## LIST OF REFERENCES

Benjamin, T. B. (1965) Significance of the Vortex Breakdown Phenomenon, *J. Basic Eng.*, June, 1965, pp. 518-524.

Deng, Q., and Gursul, I. (1997) Vortex Breakdown over a Delta Wing with Oscillating Leading Edge Flaps, *Experiments in Fluids*, No. 23, pp. 347-352.

Gursul, I., and Yang, H. (1995) On fluctuations of vortex breakdown location, *Phys. Fluids*, Vol. 7, No. 1, pp. 229-231.

Hall, M. G. (1972) Vortex Breakdown, *Annual Review of Fluid Mechanics*, Vol. 4, pp. 195-218.

Hummel, D., and Srinivasan, P. S. (1967) Vortex Breakdown Effects on the Low-speed Aerodynamic Characteristics of Slender Delta Wings in Symmetrical Flow, *Journal of the Royal Aeronautical Society*, Vol. 71, pp. 319-322.

Leibovich, S. (1978) The Structure of Vortex Breakdown, *Annual Review of Fluid Mechanics*, Vol. 10, pp.221-246.

Leibovich, S. (1984) Vortex Stability and Breakdown: Survey and Extension, *AIAA Journal*, Vol. 22, No. 9, pp. 1192-1206.

LeMay, S. P., Batill, S. M., and Nelson, R.C. (1990) Vortex Dynamics on a Pitching Delta Wing, *J. Aircraft*, Vol. 27, No. 2, pp. 131-138.

Lilley, D. G. (1977) Swirl Flows in Combustion: A Review, *AIAA Journal*, Vol. 15, No. 8, pp. 1063-1078.

Menke, M., Yang, H., and Gursul, I. (1996) Further Experiments on Fluctuations of Vortex Breakdown Location, AIAA Paper 96-0205, January 1996.

Mitchell, A. M., Barberis, D., Molton, P., and Delery, J. (2000) Oscillation of Vortex Breakdown Location and Blowing Control of Time-Averaged Location, *AIAA Journal*, Vol. 38, No. 5, pp. 793-803.



Novak, F. G. (1998) An Experimental Investigation of Vortex Breakdown in Tubes at High Reynolds Numbers, Ph.D. Dissertation, Naval Postgraduate School, Monterey, CA, September 1998.

Novak, F. and Sarpkaya, T. (2000) Turbulent Vortex Breakdown at High Reynolds Numbers, *AIAA Journal*, Vol. 38, No. 5, pp. 825-834.

Sarpkaya, T. (1971a) On Stationary and Traveling Vortex Breakdowns, *J. Fluid Mech.*, Vol. 45, part 3, pp. 545-559.

Sarpkaya, T. (1971b) Vortex Breakdown in Swirling Conical Flows, *AIAA Journal*, Vol. 9, No. 9, pp. 1792-1799.

Sarpkaya, T. (1974) Effect of the Adverse Pressure Gradient on Vortex Breakdown, *AIAA Journal*, Vol. 12, No. 5, pp. 602-607.

Sarpkaya, T. (1995) Turbulent Vortex Breakdown, *Phys. Fluids*, Vol. 7, No. 10, pp. 2301-2303.

Swithenbank, J. and Chigier, N. (1969) Vortex mixing for supersonic combustion, *Proceedings of the 12th Symposium of the Combustion Institute*, pp. 1153-1162.

Wentz, W. H., Kohlman, D. L. (1971) Vortex Breakdown on Slender Sharp-Edged Wings, *J. Aircraft*, Vol. 8, No. 3, pp. 156-161.

## INITIAL DISTRIBUTION LIST

1. Defense Technical Information Center  
Ft. Belvoir, Virginia
2. Dudley Knox Library  
Naval Postgraduate School  
Monterey, California
3. Department Chairman, Code ME  
Department of Mechanical Engineering  
Naval Postgraduate School  
Monterey, California
4. Professor T. Sarpkaya, Code ME-SL  
Department of Mechanical Engineering  
Naval Postgraduate School  
Monterey, California
5. Program Officer  
Department of Mechanical Engineering  
Naval Postgraduate School  
Monterey, California
6. ENS Jonathan S. Connelly  
Summerville, South Carolina
7. CDR Francis Novak  
Department of Naval Architecture and Ocean Engineering  
United States Naval Academy  
Annapolis, Maryland
8. Professor Michael Schultz  
Department of Naval Architecture and Ocean Engineering  
United States Naval Academy  
Annapolis, Maryland